Engineering Science and Technology, an International Journal xxx (2016) xxx–xxx

HOSTED BY

ELSEVIER

Contents lists available at ScienceDirect

Engineering Science and Technology, an International Journal

journal homepage: www.elsevier.com/locate/jestch

Full Length Article

Effect of nose radius on forces, and process parameters in hot machining of Inconel 718 using finite element analysis

Asit Kumar Parida *, Kalipada Maity

National Institute of Technology Rourkela, Mechanical Engineering Department, India

ARTICLE INFO

Article history:
Received 5 July 2016
Revised 30 September 2016
Accepted 16 October 2016
Available online xxxx

Keywords:
Hot machining
FEM
Force
Nose radius
Inconel 718

ABSTRACT

In the present work, the variation of nose radius on forces, cutting temperature, stress, has been studied using finite element modeling in hot turning operation of Inconel 718. Three values of nose radius were taken (0.4, 0.8 and 1.2 mm). Cutting force, thrust force, stress, and cutting temperature have been predicted using commercial DEFORM™ software at different cutting tool nose radius in both room and heated conditions. With the increase of tool nose radius in both room and elevated machining conditions the cutting force and thrust force increased. The cutting temperature, chip thickness and chip tool contact length also have been studied. In order to validate the numerical results an experimental analysis has been performed and good agreement between them has been observed

1. Introduction

Machining of hard materials like Nickel, Titanium and copper base alloys are the now great used in the aerospace sector, marine sector, biomedical equipment, and much more sector due to excellent properties like high indentation hardness, high abrasiveness, etc.[1]. But the removal of these materials in metal cutting operation creates a great challenge to industries due rapid tool wear. Although there are many techniques are available for machining hard materials like non-conventional machining process, hard turning, grinding etc., but there is some advantage and disadvantage of the process shown in Fig. 1. Hot machining is a method which overcomes the following above process without compromise the quality and cost. Machining of hard material using hot machining carried out by different researchers using the different heating method. Each heating methods have some disadvantage and disadvantage shown in Table 1[2]. Heating the material using different method was studied by a different researcher, Induction method [3–5], plasma heating [6–10], flame heating [11–14] etc. From the literature review, it was found that the heating of material influences the machinability.

The surface integrity, cutting forces, and the tool faces temperature affected by cutting geometry of the tool. Tool live, surface integrity is mostly influenced by the tool nose geometry was investigated by different researchers. Woon et al. [15] used finite element simulation to study the effect of nose radius on chip formation, shear stress distribution, hydrostatic stress distribution and effective rake angle in micromachining of AISI 4340 steel. They had taken four value of cutting tool nose radius (0, 1, 5, and 8). The ratio of uncut thickness and nose radius affect the chip formation process [15,16] Arif et al. [17] analyzed the change of tool nose radius on MRR(material removal rate), subsurface damage, and specific cutting energy. They found that the increase of undeformed chip thickness and Thrust changes MRR in milling. The mechanism of tool wear in thermally enhanced machining was studied by Bermingham et al. [18]. They used furnace heating method for heat the Ti-6Al-4V work material and taken 30 °C, 150 °C, 250 °C and 350 °C as material removal temperature. At 350 heating temperature cutting force decreased, but tool wear increased. For validate to this result, a finite element simulation has been carried out by Xi et al. [19] using ABAQUS software.

Yang et al. studied the cutting temperature generation in micro end milling process of Al2024-T6 with WC micro cutter using finite element method [20]. Saedon et al. studied the finite element analysis of micro machining and macro machining, the effect of nose radius on chip thickness on machining [21]. Liu et al. analyzed ductile cutting of silicon wafers using different cutting noses. It was found that the critical value of uncut chip thickness changes with the cutting noses and linear relationship between the uncut chip thickness and cutting noses [22].

A numerical modeling was reported by Wu et al. in micro turning machining operation using different nose radius. The cutting

* Corresponding author.
E-mail address: Email-asitzone4u@gmail.com (A.K. Parida).
Peer review under responsibility of Karabuk University.

http://dx.doi.org/10.1016/j.jestch.2016.10.006
2215-0986/

Please cite this article in press as: A.K. Parida, K. Maity, Effect of nose radius on forces, and process parameters in hot machining of Inconel 718 using finite element analysis, Eng. Sci. Tech., Int. J. (2016), http://dx.doi.org/10.1016/j.jestch.2016.10.006

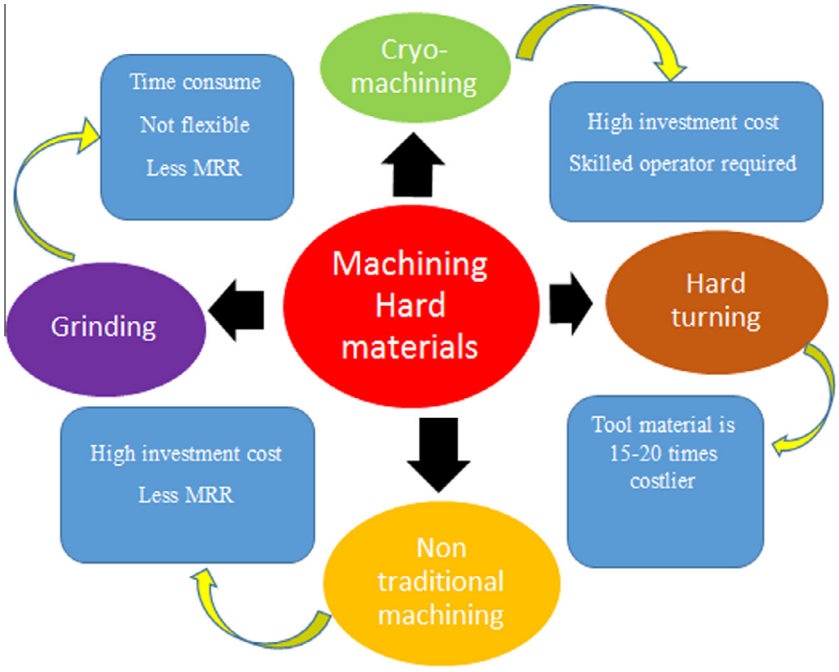

Fig. 1. Different machining process used for machining hard materials.

Table 1
Heat source/Heating Method Used.

Heat source	Advantage	Disadvantage
Laser	Local heat concentration Delicate shape machining	High investment cost Not able to all materials
Induction coil	Easy to use Heat can be imposed through	Low penetration of heat Tool mobility is not possible
Gas flame	Simple design	Low on penetration of heat Titanium alloy reacts with the tool material
Plasma	Local heat concentration	Cannot control accurately
Electricity	Simple equipment Low cost investment	Cannot control accurately

force and specific cutting force were greatly affected by the grain size. It was found that higher cutting force and specific cutting energy obtained on the smaller variation of grain size [22]. The wear of cutting tool and how it is affected by cutting tool nose radius was studied by Rech et al. using PM-HSS milling inserts. Numerical modeling also carried out to validate the experimental results. The formation chip in metal cutting operation with curvilinear nose tools and its mechanism was analyzed by Karpat and Ozel [23]. Chamfered nose along with different nose designs was taken for machining AISI 4340 steel using PCBN tools. They found that mechanics of machining was immensely affected by the size of cutting nose. The residual stresses were also reported by many researchers using different nose radius value [24–27].

But a little work was found Preparation of nose radius in the hot machining process. Among all heating method gas flame heating is simple and cheap compared to another heating process, so the present work is based on the effect of nose radius on hot machining using FE analysis. The aim of the study is to analyze the preparation of noses on temperature distribution on the tool and process variables. Investigations of the preparation of noses with different machining conditions were carried out in both conventional and hot turning operation. Analyze the effects of the process variables like temperature distribution of tool, stress, strain using finite element simulation.

2. Experimental work

All tests were performed on a center Lathe for both room temperature and preheating machining conditions. The workpiece Inconel 718 (Diameter 50 mm and 300 mm length) in the form of round bar and hardness of 43 HRC as received from the supplier. Tables 2 and 3 shows the workpiece material composition and Thermomechanical properties of Inconel 718. It is found in the literature review that the shear strength of Inconel start decreases when the heating temperature around 600 °C [28]. So in this study, the 600 °C temperature has been taken for simulation and experimental study. The experimental and schematic diagram for hot machining is illustrated in Fig. 2.

The temperature of workpiece surface was measured with the help of thermocouple (K-type) range of (200–1200 °C). The flow

Table 2
Chemical composition of Inconel 718[29].

Ni	Fe	Cr	Cb	Mo	Ti	Al	C	S
53.46	18.31	18.29	4.97	3.01	1.02	0.52	0.015	0.0004

Table 3
Thermo-mechanical properties of Inconel 718 and WC[30].

Properties	Inconel 718	WC
Density (kg/m^3)	8080 (kg/m^3)	15,000
Thermal conductivity (W/m/°C)	10.5 (W/m/°K)	46
Specific heat (J/kg/)	515 (J/kg°K)	203
Melting Temperature (°C)	1336	2870
Thermal Expansion (mm.mm^{-1}°/C)	13	4.7×10^{-6}

Please cite this article in press as: A.K. Parida, K. Maity, Effect of nose radius on forces, and process parameters in hot machining of Inconel 718 using finite element analysis, Eng. Sci. Tech., Int. J. (2016), http://dx.doi.org/10.1016/j.jestch.2016.10.006

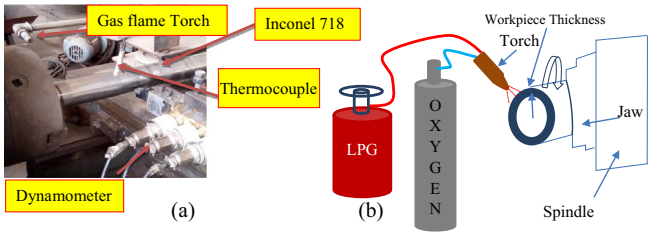

Fig. 2. Experimental (a) Schematic diagram of Hot Machining setup.

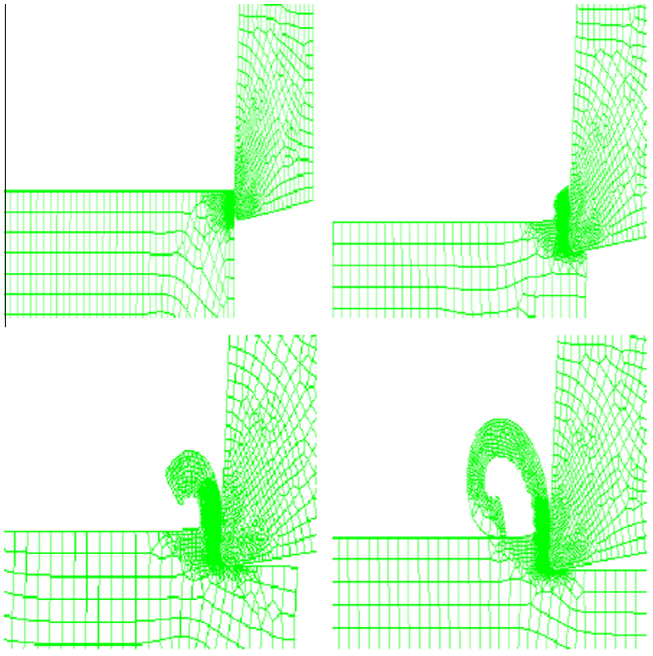

Fig. 3. Remeshing in machining simulation.

of oxygen and liquefied petroleum gas (LPG) from the cylinder was kept control so that there no interrupted in heating on the workpiece surface [13]. In order to perform the orthogonal cutting operation, the workpiece was drilled and then bored with boring tool. The experimental are carried out with varying different parameters and tabulated in Table 3. The forces were measured by the dynamometer. The chip temperature was measuered with the help of infrared pyrometer, whereas, chip thickness and chip-tool contact length were measured with the help of optical microscope respectively.

3. Finite element modeling of machining

The FEM simulation package DEFORM 2D V10.0 (SFTC 2009) was used for heat assisted machining process [31]. DEFORM software is an updated Lagrangian formulation having remeshing technique which has an advantage during machining processes. Remeshing avoid convergences and contact problem of long chips as shown in Fig. 3. The workpiece is modeled as plastic with mesh 30,000 tetrahedral elements and tool as rigid with 14,000 elements. A high mesh density was assign in the primary deformation zone with element size 0.01 mm. The workpiece dimension was assigned length 3 mm and height of 0.7 mm in the model. The thermal and velocity boundary condition was assigned to the tool and workpiece is shown in Fig. 4. The left and bottom side of the workpiece and top and right side of the tool was kept at room temperature as these surface are far away from the cutting area whereas top and right side of the workpiece and left and bottom side of the cutting tool exchange heat to the environment. The bottom portion of the workpiece was restricted to y-direction movement whereas the cutting tool was fixed in both x and y-direction.

In order to simulate the effect of hot machining, a heat exchange window is available in DEFORM software to define heat exchange in the local area and moves along the workpiece. The environment temperature was set at 30 °C, except for a spot (called the nozzle radius) which is kept at the heating temperature 600 °C. The total heat input, Q, through the window can be defined in Eq. (1). as

$$Q = hA(T_{window} - T_{workpiece}) \tag{1}$$

where A is the surface area of heat exchange window, h is the convention coefficient, T_{window} and $T_{workpiece}$ are the temperature of the window and workpiece respectively. Within the aforementioned window, both tool and workpiece might exchange heat to the environment.

3.1. Work material modeling

The material model of Inconel 718 imported from the DEFORM library [27]. The Thermo-mechanical properties of workpiece and tungsten carbide are shown in Table 4. The constitutive equation for Johnson-cook model is defined in Eq. (2). Other researchers applied Johnson material modeling in thermal assisted machining for simulation [32,33].

$$\bar{\sigma} = (A + B(\bar{\varepsilon})^n)\left(1 + c\ln\left(\frac{\dot{\bar{\varepsilon}}}{\dot{\bar{\varepsilon}}_0}\right)\right)\left(1 - \left(\frac{T - T_r}{T_m - T_r}\right)^m\right) \tag{2}$$

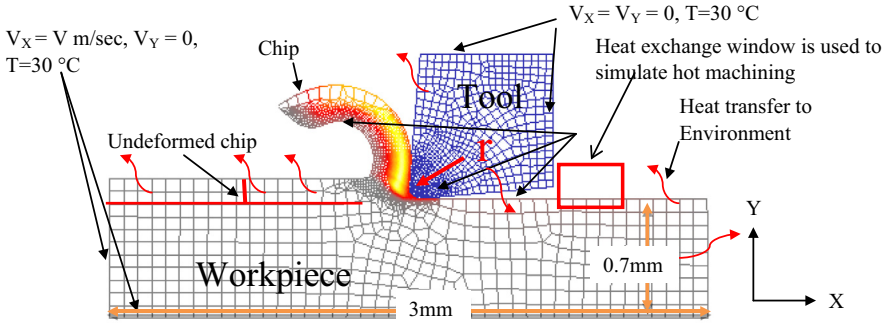

Fig. 4. Displacement and thermal boundary conditions of the workpiece and tool, r is tool nose radius.

Please cite this article in press as: A.K. Parida, K. Maity, Effect of nose radius on forces, and process parameters in hot machining of Inconel 718 using finite element analysis, Eng. Sci. Tech., Int. J. (2016), http://dx.doi.org/10.1016/j.jestch.2016.10.006

Table 4
Experimental conditions used in the room and elevated temperature.

Machine Tool	Center Lathe, 6.5 hp
Work specimen	Inconel 718
Cutting tool	TNMG
Hardness	43HRC
Dimension	50 x 300 mm
Insert	Uncoated carbide
Cutting speed	40, 100 m/min
Feed rate	0.13 mm/rev
Depth of cut	0.8 mm
Nose radius	0.4, 0.8, and 1.2 mm

A, B, and C are Johnson-cook material constant at room temperature. m and n are constant called thermal softening and hardening coefficient [30]. $\bar{\varepsilon}$, $\dot{\bar{\varepsilon}}$, $\dot{\bar{\varepsilon}}_0$ represents the plastic strain, plastic strain rate, and reference strain rate. T is the temperature, Tm, and Tr are the workpieces melting and room temperature respectively

3.2. Friction model

For Chip-tool friction, simple shear friction model was used and defined in Eq. (3)

$$\tau = mk_{chip} \tag{3}$$

The value of shear friction factor (m = 1) was taken [34] and k_{chip} chip material yield strength near the tool-chip interface

3.3. Fracture Model

Fracture criteria which cause separation of chip is implemented in this study. Nickel base alloys at low cutting speeds produce segment types of chips. Cockcroft and Latham was implemented in DEFORM software is shown in Eq. (4)

$$\int_0^{\varepsilon_f} \sigma_1 d\varepsilon = D \tag{4}$$

where ε_f the effective strain, σ_1 is maximum principal stress and D is material constant [34].

4. Result and discussion

The effect of nose radius of the tool on cutting and Thrust force, temperature, stress, were discussed.

4.1. Effect of variation of nose radius of tool on cutting and thrust force

The cutting and thrust force reaches steady state after 2 mm in both room and heating simulation. The cutting and thrust force reduced 12,6, 12% and 34,14, 23% at 0.4, 0.8 and 1.2 mm nose radius respectively compared to room temperature conditions at heating temperature of 600 °C. This is due to thermal softening of the material due to external heating. The comparison between the simulated and experimental cutting force and thrust force at room temperature with different nose radius is shown in Fig. 5 and Fig. 6 respectively. Whereas in heating temperature (600 °C) cutting and thrust increases with the increase of nose radius at room and heating temperature (Fig. 7). There are many reason for this, first with increase of nose radius, increase of bluntness of tool is more, which cause larger force in plastic deformation. Another reason is that the tool tip contact is larger with increase of nose radius which increase the specific cutting energy i.e. cutting force. In all tests, the thrust forces show larger value than the cutting force. Similar observation was noticed by researcher [35].

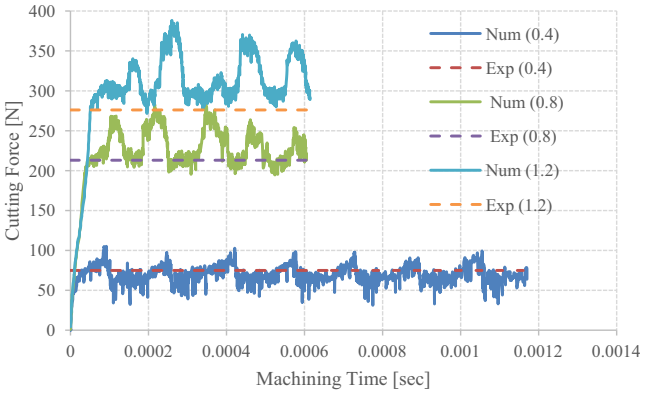

Fig. 5. Comparison between the simulated and experimental cutting force at room temperature with different nose radius.

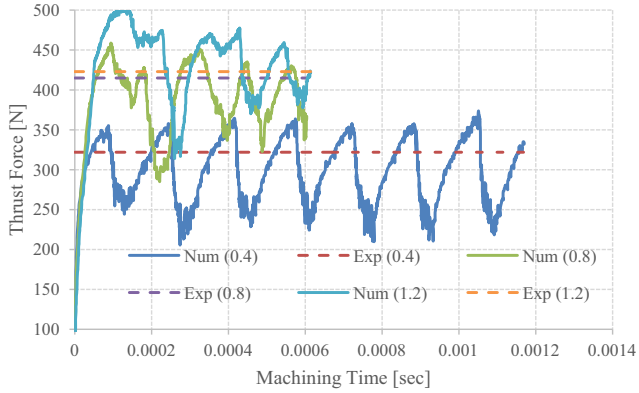

Fig. 6. Comparison between the experimental and simulated thrust force at room temperature at different nose radius.

Increase of nose radius decrease the shear angle and increase the chip thickness which is responsible for large shear plane in primary deformation zone [20]. Increasing the cutting speed from 40 m/min to 100 m/min there was decrease of cutting and Thrust force at room and heating temperature conditions. The cutting and Thrust force at nose radius of 0.8 mm was slightly overestimated whereas at 0.4 and 1.2 mm nose radius simulated shows good agreement with the experimental values. The error% between the simulated and experimental result may be due to mesh size, friction model, and material modeling [17].

4.2. Influences of heating temperature on process zone temperature, chip formation and stress

The effect of heating temperature on the process zone temperature, chip formation and stress is shown in Fig. 8. The process zone temperature at 600 °C heating conditions increased 1050 °C compared 985 °C to room temperature conditions at nose radius 0.4 mm and cutting speed of 40 m/min. The application of external heat imposed to the workpiece surface increase the temperature at the process/shear/cutting zone by lowering shear cutting energy and reduce friction between the chip and tool in secondary zone due to plastic deformation, which helps on reducing cutting force and stress during machining. At room temperature the chip produce is segmented type due to fluctuation of forces, whereas at heating temperature of 600 °C the chip formed is continues type due to no fluctuation of forces (Fig. 7).

Similar observation was observed [36,37] in thermal assisted machining. But increase of nose radius, may chance of breakage

Please cite this article in press as: A.K. Parida, K. Maity, Effect of nose radius on forces, and process parameters in hot machining of Inconel 718 using finite element analysis, Eng. Sci. Tech., Int. J. (2016), http://dx.doi.org/10.1016/j.jestch.2016.10.006

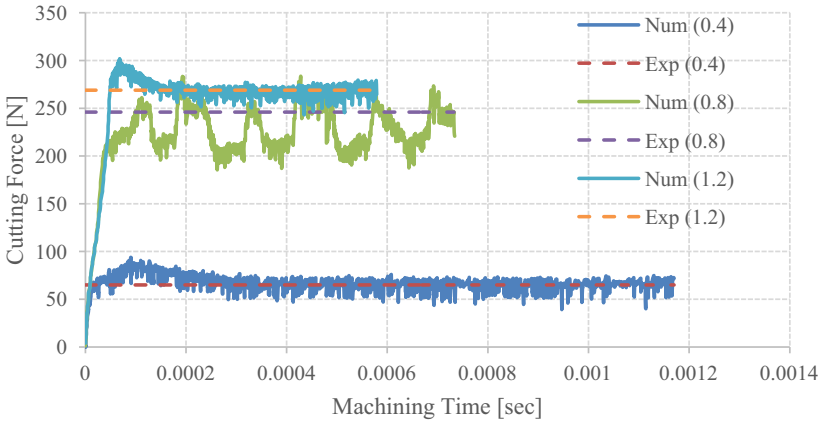

(a)

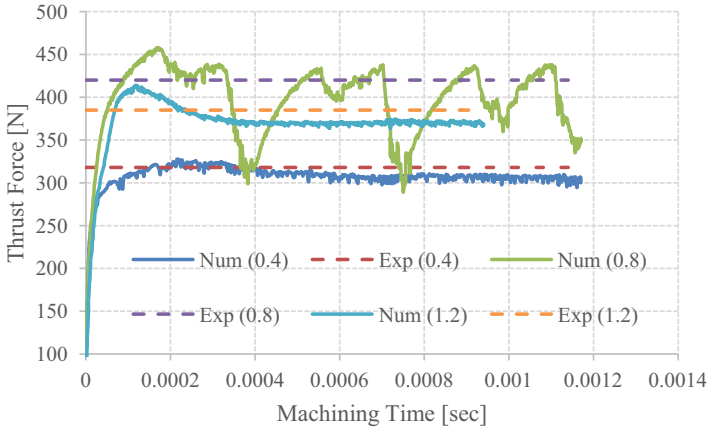

(b)

Fig. 7. Comparison between Numerical and Experimental Cutting (a) and Thrust force (b) at T = 600 °C,

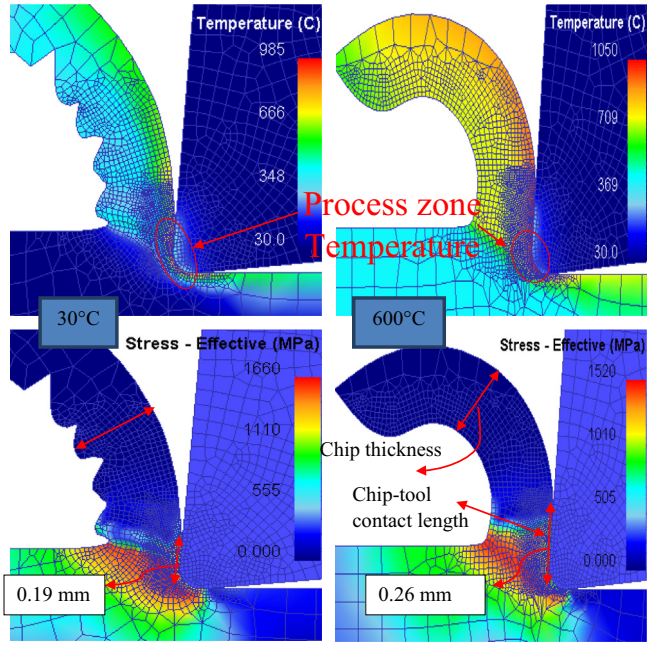

Fig. 8. Effective stress distribution process zone temperature at room and heating condition at nose radius 0.4 mm.

of tool tip which cause rise on temperature on the nose of cutting tool thus reduce increase of cutting force. It was also noticed that the temperature of the chip increased at heated conditions compared to room temperature conditions as per Fig. 8 at steady state cutting conditions. In order to validate the chip temperature an infrared pyrometer was utilized during the machining and positive coherence with the simulated temperature was observed as shown in Fig. 9. It was observed that no big variation of chip temperature of chip with increase of nose radius of the cutting tool.

The effective stress reduces from room temperature to heating temperature of 600 °C was 1660 MPa to1520 MPa, at nose radius 0.4 mm and cutting speed of 40 m/min. The increased of nose radius increase the flow stress because of flank wear formation at higher nose radius. The reduction of stress at heating conditions confirm that reduction of cutting force at heating temperature compared due to heating on the workpiece surface. The reduction of flow stress due to rise in temperature at shear zone in heating conditions. Similar observation was observed in laser heating machining of hard material [38].

4.3. Effect of nose radius on chip thickness and chip-tool contact length with respect to heating temperature

It was observed, increase of heating temperature reduced the chip thickness and increased the chip-tool contact length

Please cite this article in press as: A.K. Parida, K. Maity, Effect of nose radius on forces, and process parameters in hot machining of Inconel 718 using finite element analysis, Eng. Sci. Tech., Int. J. (2016), http://dx.doi.org/10.1016/j.jestch.2016.10.006

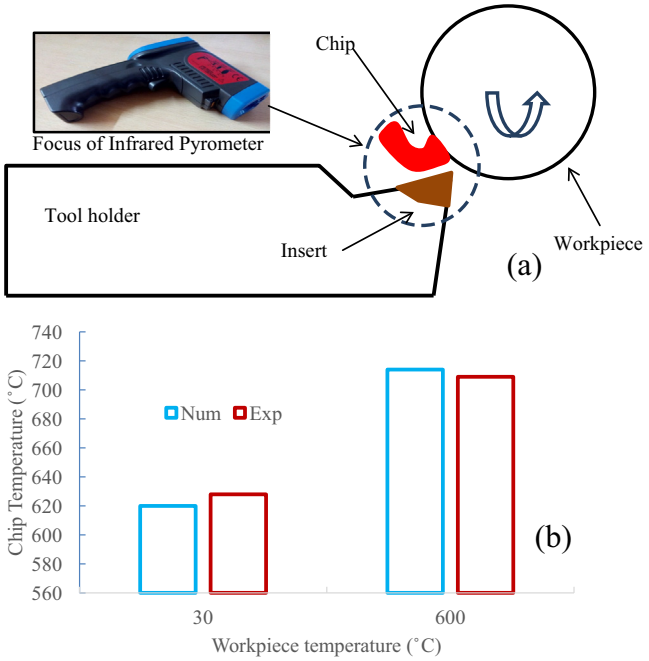

Fig. 9. Schematic diagram for measurement of the temperature (a) Comparison between the numerical and experimental temperature at cutting speed of 40 m/min, nose radius of 0.4 mm.

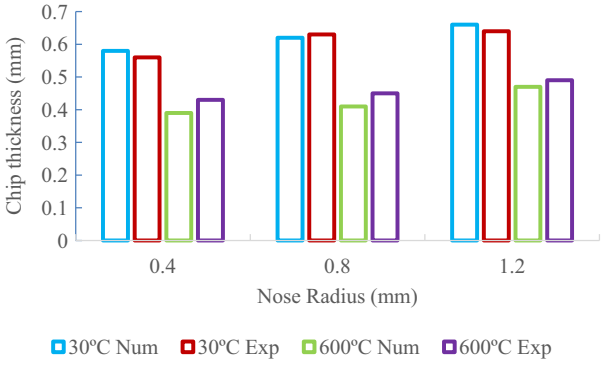

Fig. 10. Comparison between the Numerical and Experimental chip thickness at room and heating conditions.

compared to in room temperature. The chip-tool contact length and chip thickness were measured from the simulation image (Fig. 8). The increase of nose radius; there was increased of chip thickness and the chip-tool contact length compared to room temperature machining conditions. Similarly, the experimental chip thickness and chip-tool contact length were measured with the help of the optical microscope. The comparison between the experimental and numerical chip thickness is shown in Fig. 10 and maximum error of 3% and 10% at 30 °C and 600 °C temperature was observed.

The increase of chip-tool contact length has many advantages. It shifts the hot spot away from the cutting nose and lower the stress acting on the tool. The optical image of chip tool contact length and comparison between the experimental and simulated chip tool contact length is presented as Fig. 11. Maximum error% between experiment and simulated value are 15% and 11% at 30 °C and 600 °C heating temperature respectively.

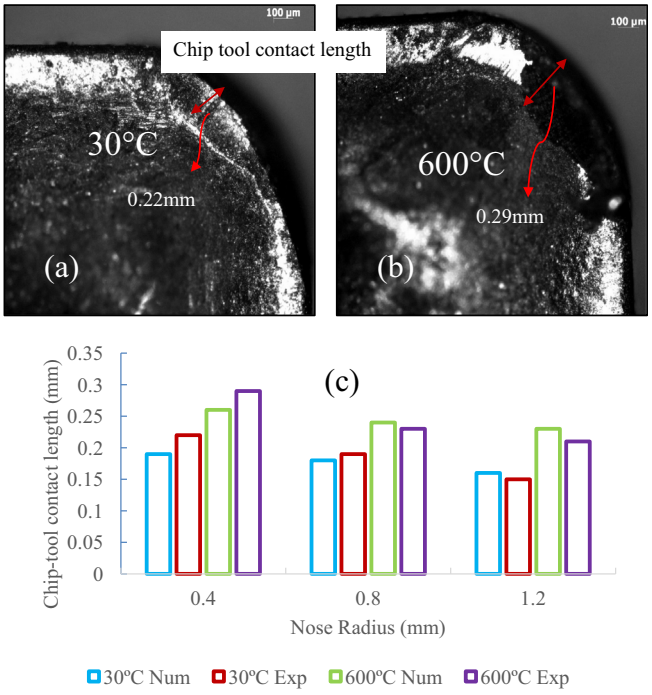

Fig. 11. Optical view of Chip tool contact length at (a) 30 °C (b) 600 °C at nose radius 0.4 mm (c) Comparison between the Numerical and Experimental chip-tool contact length at workpiece temperature and different nose radius conditions.

5. Conclusions

Machining of Inconel 718 in the room and elevated temperature is analyzed using both experimentally and finite element simulation presented in this paper. Cutting force, thrust force, temperature, chip shape, and size analyzed both in room and elevated temperature. The simulation results are partially validated with the experimental values. Finite element analysis is the best tools which can predict stress, strain, and temperature, which is not measurable in experimentally and time-consuming. The information of these parameters gives a clear understanding of the physics of machining processes. Application of heat in close proximity to the surface of the workpiece can significantly reduce the cutting and Thrust force. The increase of process zone temperature reduces heat generation which reduce flow stress and cutting force in hot machining compared to room temperature machining processes. The chip thickness size was decreased and chip tool contact increased with increase of workpiece temperature and nose radius. The predicted results show good correlation to the experimental results.

References

[1] K. Nakayama, M. Arai, T. Kanda, Machining characteristics of hard materials, CIRP Ann. Manuf. Technol. 37 (1988) 89–92, http://dx.doi.org/10.1016/S0007-8506(07)61592-3.
[2] E. Rahim, N. Warap, Z. Mohid, Thermal-Assisted Machining of Nickel-based Alloy, Intech Publication, http://dx.doi.org/10.5772/61101.
[3] M.A. Lajis, A.K.M.N. Amin, A.N.M. Karim, H.C.D.M. Radzi, T.L. Ginta, Hot machining of hardened steels with coated carbide inserts, Am. J. Eng. Appl. Sci. 2 (2009) 421–427, http://dx.doi.org/10.3844/ajeassp.2009.421.427.
[4] M. Baili, V. Wagner, G. Dessein, J. Sallaberry, D. Lallement, An experimental investigation of hot machining with induction to improve Ti-5553 machinability, Appl. Mech. Mater. 62 (2011) 67–76, http://dx.doi.org/10.4028/www.scientific.net/AMM.62.67.
[5] M.A. Lajis, A.K.M. Nurul Amin, A.N.M. Karim, Surface integrity in hot machining of AISI D2 hardened steel, Adv. Mater. Res. 500 (2012) 44–50, http://dx.doi.org/10.4028/www.scientific.net/AMR.500.44.

Please cite this article in press as: A.K. Parida, K. Maity, Effect of nose radius on forces, and process parameters in hot machining of Inconel 718 using finite element analysis, Eng. Sci. Tech., Int. J. (2016), http://dx.doi.org/10.1016/j.jestch.2016.10.006

[6] T. Kttagawa, K. Maekawa, Plasma hot machining for new engineering materials, Wear 139 (1990) 251–267, http://dx.doi.org/10.1016/0043-1648(90)90049-G.
[7] C.E. Leshock, J.N. Kim, Y.C. Shin, Plasma enhanced machining of Inconel 718: modeling of workpiece temperature with plasma heating and experimental results, Int. J. Mach. Tools Manuf. 41 (2001) 877–897, http://dx.doi.org/10.1016/S0890-6955(00)00106-1.
[8] B.K. Hinds, S.M. De Almeida, Plasma arc heating for hot machining, Int. J. Mach. Tool Des. Res. 21 (1981) 143–152, http://dx.doi.org/10.1016/0020-7357(81)90005-6.
[9] L.N. López de Lacalle, J.A. Sánchez, A. Lamikiz, A. Celaya, Plasma assisted milling of heat-resistant superalloys, J. Manuf. Sci. Eng. 126 (2004) 274, http://dx.doi.org/10.1115/1.1644548.
[10] J.W. Novak, Y.C. Shin, F.P. Incropera, Assessment of plasma enhanced machining for improved machinability of Inconel 718, J. Manuf. Sci. Eng. 119 (1997) 125, http://dx.doi.org/10.1115/1.2836550.
[11] K.P. Maity, P.K. Swain, An experimental investigation of hot-machining to predict tool life, J. Mater. Process. Technol. 198 (2008) 344–349, http://dx.doi.org/10.1016/j.jmatprotec.2007.07.018.
[12] N. Tosun, L. Özler, A study of tool life in hot machining using artificial neural networks and regression analysis method, J. Mater. Process. Technol. 124 (2002) 99–104, http://dx.doi.org/10.1016/S0924-0136(02)00086-9.
[13] L. Özler, A. Inan, C. Özel, Theoretical and experimental determination of tool life in hot machining of austenitic manganese steel, Int. J. Mach. Tools Manuf. 41 (2001) 163–172, http://dx.doi.org/10.1016/S0890-6955(00)00077-8.
[14] D.K. Pal, S.K. Basu, Hot machining of austenitic manganese steel by shaping, Int. J. Mach. Tools Res. 11 (1971) 45–61.
[15] K.S. Woon, M. Rahman, F.Z. Fang, K.S. Neo, K. Liu, Investigations of tool edge radius effect in micromachining: a FEM simulation approach, J. Mater. Process. Technol. 195 (2008) 204–211, http://dx.doi.org/10.1016/j.jmatprotec.2007.04.137.
[16] K.S. Woon, M. Rahman, The effect of tool edge radius on the chip formation behavior of tool-based micromachining, Int. J. Adv. Manuf. Technol. 50 (2010) 961–977, http://dx.doi.org/10.1007/s00170-010-2574-x.
[17] M. Arif, M. Rahman, W.Y. San, A study on the effect of tool-edge radius on critical machining characteristics in ultra-precision milling of tungsten carbide, Int. J. Adv. Manuf. Technol. 67 (2013) 1257–1265, http://dx.doi.org/10.1007/s00170-012-4563-8.
[18] M.J. Bermingham, S. Palanisamy, M.S. Dargusch, Understanding the tool wear mechanism during thermally assisted machining Ti-6Al-4V, Int. J. Mach. Tools Manuf. 62 (2012) 76–87, http://dx.doi.org/10.1016/j.ijmachtools.2012.07.001.
[19] Y. Xi, M. Bermingham, G. Wang, M. Dargusch, FEA modelling of cutting force and chip formation in thermally assisted machining of Ti6Al4V alloy, Mater. Sci. Forum. 765 (2013) 343–347, http://dx.doi.org/10.4028/www.scientific.net/MSF.765.343.
[20] Y.C. Yen, A. Jain, T. Altan, A finite element analysis of orthogonal machining using different tool edge geometries, J. Mater. Process. Technol. 146 (2004) 72–81, http://dx.doi.org/10.1016/S0924-0136(03)00846-X.
[21] J. Saedon, Micromilling of hardened (62 HRC) AISI D2 cold, WORK (2011).
[22] K. Liu, X.P. Li, M. Rahman, K.S. Neo, X.D. Liu, A study of the effect of tool cutting edge radius on ductile cutting of silicon wafers, Int. J. Adv. Manuf. Technol. 32 (2007) 631–637, http://dx.doi.org/10.1007/s00170-005-0364-7.
[23] Y. Karpat, T. Özel, Mechanics of high speed cutting with curvilinear edge tools, Int. J. Mach. Tools Manuf. 48 (2008) 195–208, http://dx.doi.org/10.1016/j.ijmachtools.2007.08.015.
[24] K.C. Ee, O.W. Dillon, I.S. Jawahir, Finite element modeling of residual stresses in machining induced by cutting using a tool with finite edge radius, Int. J. Mech. Sci. 47 (2005) 1611–1628, http://dx.doi.org/10.1016/j.ijmecsci.2005.06.001.
[25] J. Hua, R. Shivpuri, X. Cheng, V. Bedekar, Y. Matsumoto, F. Hashimoto, et al., Effect of feed rate, workpiece hardness and cutting edge on subsurface residual stress in the hard turning of bearing steel using chamfer + hone cutting edge geometry, Mater. Sci. Eng. A. 394 (2005) 238–248, http://dx.doi.org/10.1016/j.msea.2004.11.011.
[26] A.R.C. Sharman, J.I. Hughes, K. Ridgway, The effect of tool nose radius on surface integrity and residual stresses when turning Inconel 718™, J. Mater. Process. Technol. 216 (2015) 123–132, http://dx.doi.org/10.1016/j.jmatprotec.2014.09.002.
[27] P.I. Varela, C.S. Rakurty, A.K. Balaji, Surface integrity in hard machining of 300M Steel: effect of cutting-edge geometry on machining induced residual stresses, Procedia CIRP 13 (2014) 288–293, http://dx.doi.org/10.1016/j.procir.2014.04.049.
[28] S. Sun, M. Brandt, M.S. Dargusch, Thermally enhanced machining of hard-to-machine materials: a review, Int. J. Mach. Tools Manuf. 50 (2010) 663–680, http://dx.doi.org/10.1016/j.ijmachtools.2010.04.008.
[29] B. Shi, H. Attia, R. Vargas, S. Tavakoli, Numerical and experimental investigation of laser-assisted machining of Inconel 718, Machining Science and Technology, http://dx.doi.org/10.1080/10910340802523314.
[30] T. Ozel, I. Lianos, J. Soriano, P.J. Arrozola, 3D finite element modelling of chip formation process for machining Inconel 718 : comparison of FE software predictions, Machining Science and Technology 37–41, http://dx.doi.org/10.1080/10910344.2011.557950.
[31] DEFORM 2D Version 10, User Manual, SFTC, Columbus, Ohio State, USA.
[32] S. Joshi, A. Tewari, S.S. Joshi, Microstructural characterization of chip segmentation under different machining environments in orthogonal machining of Ti6Al4V, J. Eng. Mater. Technol. 137 (2015) 11005, http://dx.doi.org/10.1115/1.4028841.
[33] Y. Xi, M. Bermingham, G. Wang, M. Dargusch, SPH/FE modeling of cutting force and chip formation during thermally assisted machining of Ti6Al4V alloy, Comput. Mater. Sci. 84 (2014) 188–197, http://dx.doi.org/10.1016/j.commatsci.2013.12.018.
[34] S. Caruso, S. Imbrogno, G. Rotella, M.I. Ciaran, P.J. Arrazola, L. Filice, et al., Numerical simulation of surface modification during machining of nickel-based superalloy, Procedia CIRP. 31 (2015) 130–135, http://dx.doi.org/10.1016/j.procir.2015.03.053.
[35] M. Liu, J.I. Takagi, A. Tsukuda, Effect of tool nose radius and tool wear on residual stress distribution in hard turning of bearing steel, J. Mater. Process. Technol. 150 (2004) 234–241, http://dx.doi.org/10.1016/j.jmatprotec.2004.02.038.
[36] S. Joshi, A. Tewari, S. Joshi, Influence of preheating on chip segmentation and microstructure in orthogonal machining of Ti6Al4V, J. Manuf. Sci. Eng. 135 (2014) 1–11, http://dx.doi.org/10.1115/1.4025741.
[37] R. Muhammad, A. Maurotto, A. Roy, V.V. Silberschmidt, Hot ultrasonically assisted turning of β-Ti alloy 1 (2012) 336–341, http://dx.doi.org/10.1016/j.procir.2012.04.060.
[38] G. Singh, M. Teli, A. Samanta, R. Singh, G. Singh, et al., Materials and Manufacturing Processes Finite Element Modeling of Laser-Assisted Machining of AISI D2 Tool Steel Finite Element Modeling of Laser-Assisted Machining of AISI D2 Tool Steel, (2013) 37–41. doi:10.1080/10426914.2012.700160.

Please cite this article in press as: A.K. Parida, K. Maity, Effect of nose radius on forces, and process parameters in hot machining of Inconel 718 using finite element analysis, Eng. Sci. Tech., Int. J. (2016), http://dx.doi.org/10.1016/j.jestch.2016.10.006